Twelve receptor molecules attach per viral particle of human rhinovirus serotype 2 via multiple modules

Tünde Konecsni[a,b], Leopold Kremser[a], Luc Snyers[c,1], Christian Rankl[d], Ferenc Kilár[b], Ernst Kenndler[a], Dieter Blaas[c,*]

[a]*Institute for Analytical Chemistry, University of Vienna, Währingerstr. 38, A 1090 Vienna, Austria*
[b]*Institute of Bioanalysis, University of Pécs, Faculty of Medicine, Szigeti út 12. H 7624 Pécs, Hungary*
[c]*Max F. Perutz Laboratories, University Departments at the Vienna Biocenter, Department of Medical Biochemistry, University of Vienna, Dr. Bohr Gasse 9/3, A-1030 Vienna, Austria*
[d]*Institute for Biophysics, J. Kepler University, Altenberger Str. 69, A-4040 Linz, Austria*

Received 23 March 2004; revised 4 May 2004; accepted 12 May 2004

Available online 20 May 2004

Edited by Hans-Dieter Klenk

Abstract The crystallographic $T = 1$ (pseudo $T = 3$) icosahedral symmetry of the human rhinovirus capsid dictates the presence of 60 identical, symmetry related surface structures that are available for antibody and receptor binding. X-ray crystallography has shown that 60 individual very-low density lipoprotein receptor (VLDLR) modules bind to HRV2. Their arrangement around the fivefold axes of the virion suggested that tandem oligomers of such modules could attach simultaneously to symmetry-related sites. By resolving virus particles carrying various numbers of artificial recombinant concatemers of VLDLR repeat 3 (V33333) by capillary electrophoresis and extrapolation of the measured mobilities to that at saturation of all binding sites, we present evidence for up to 12 molecules of the concatemer to bind one single virion.

Keywords: Capillary electrophoresis; Human rhinovirus; Picornavirus; Receptor; Low-density lipoprotein; Very low-density lipoprotein; Structure

1. Introduction

Human rhinoviruses (HRVs), main causative agents of common cold infections, belong to the family of *picornaviridae* [1]. They are composed of four individual capsid proteins, VP1, VP2, VP3, and VP4, and a single stranded RNA genome of messenger sense polarity with about 7100 bases. There are 60 copies of each of the VPs in one viral particle. These proteins are arranged in a $T = 1$, pseudo $T = 3$ icosahedral symmetry. Whereas VP4 is a small (7 kDa), internal protein residing close to the RNA, the remaining capsid proteins fold into β-barrel structures with the connecting loops exposed at the surface. The amino acid sequence of these loops is highly variable giving rise to more than 100 antigenically distinguishable serotypes. These are divided into a minor (10 serotypes) and a major (91 serotypes) group based on their specific binding to members of the low-density lipoprotein receptor (LDLR) family or to intercellular adhesion molecule 1 (ICAM-1), respectively [2]. Another more recent classification into genus A and B is based on sequence similarity [3].

The LDLR family comprises LDLR proper, the prototype of the family, very-low density lipoprotein receptor (VLDLR), the LDLR related protein (LRP) and a number of other endocytic receptors with some also being involved in signal transduction [4]. Minor group HRVs attach to LDLR, VLDLR, and LRP for cell entry [5,6]. LDL-receptors are mosaic proteins that most probably evolved from single modules and building blocks. Their ligand-binding domains at the N-terminus are composed of various numbers of ligand binding repeats or type A modules, each about 40 amino acids in length, among them six cysteines that are all engaged in disulfide bridges. This structure is further stabilized by a Ca^{2+} ion chelated by an acidic cluster that is composed from highly conserved aspartic and glutamic acid residues. LDLR has seven such modules, VLDLR has eight, and LRP has clusters of 2, 8, 10, and 11 ligand binding repeats. C-terminal to these domains are sequences with similarity to the epidermal growth factor receptor, a β-propeller with YWTD motives, a more or less O-glycosylated membrane proximal domain, a transmembrane domain and a cytoplasmic tail with NPXY adapter binding sequences [7] responsible for clathrin-mediated endocytosis [8].

In order to determine the binding site of these receptors on the viral surface, we have previously constructed several forms of truncated soluble receptors just containing the N-terminal ligand binding domain or parts of it [9]. Using these bacterially expressed derivatives of VLDLR, complexes with HRV2, a prototype of the minor receptor group of HRVs, were assembled and analyzed by cryo-electron microscopy and X-ray crystallography [10–12]. The derived structures showed that single V3 modules (repeat #3 of VLDLR) attached to the BC and HI loop of VP1 close to the fivefold axis of icosahedral symmetry (see Fig. 5). This suggested the possibility of multi-module attachment; the arrangement of the C- and N-termini of the single modules is such as to evoke that more than one module, when present within either the native receptor or within artificial concatemers, might attach simultaneously to more than one binding site. This was also suggested by the

* Corresponding author. Fax: +43-1-4277-9616.
E-mail address: dieter.blaas@meduniwien.ac.at (D. Blaas).

[1] Present address: Institute of Histology and Embryology, University of Vienna, Schwarzspanierstrasse 17, A-1090 Vienna, Austria.

0014-5793/$22.00
doi:10.1016/j.febslet.2004.05.015

increase in the virus neutralizing potential of soluble receptor derivatives upon concatenation of individual modules [12,13]. When incubated with virus prior to challenging HeLa cells, soluble receptors attach to the virus, compete for the binding sites on the cell surface and thereby protect the cells against virus infection [14,15].

We have previously determined the stoichiometry of MBP-V1-3 and of MBP-V1-8 when complexed with HRV2 and estimated the affinities of the binding reaction by capillary electrophoresis (CE) [16]. These proteins are fusions of maltose binding protein and parts (MBP-V1-3) and the entire (MBP-V1-8) ligand binding domain of VLDLR fused to maltose binding protein (MBP) at the N-terminus, for better folding, and to a his tag, to aid purification, at the C-terminus [9]. For these receptors a stoichiometry of 1:60 and 1:30, respectively, was found [16]. Since the receptor-binding site was not known, this was taken to suggest attachment of the receptor via a putative pseudo twofold axis created by a kink in the structure [17] over a twofold symmetry axis of the virus. The structures of complexes between HRV2 and a number of receptor fragments and artificial concatemers being now available [10], it is clear that the receptor modules bind at the fivefold axes of viral symmetry. In order to assess whether more modules within a single receptor molecule can attach to the virus, we attempted to determine the stoichiometry of the reaction between HRV2 and a concatemer of five copies of repeat 3 (MBP-V33333) of VLDLR by the same CE methodology. During this work, we observed that, at low receptor: virus ratio, CE resolved complexes with different stoichiometry. At higher ratios, the resolution diminished and at large excess of receptor, single peaks, corresponding to the saturated complex and to free receptor, were seen. The mobilities of the peaks decreased non-linearly with an increase in viral occupancy. Nevertheless, extrapolation to saturation was possible and a stoichiometry of 12 receptor molecules per virion was obtained.

2. Materials and methods

2.1. Virus and receptor preparations

HRV2, originally obtained from the American Type Culture Collection, Manassas, VA, USA, was produced and purified from infected cell pellets as described previously [11]. Purified virus in the pellet obtained after ultracentrifugation was suspended in 50 mM Tris–HCl, pH 7.4, and kept at −80 °C until use. The concentration was determined spectrophotometrically using an extinction coefficient of 7.7 at 260 nm (A_{260}) for a 1 mg/ml solution [18] corrected for contaminants with absorption at 260 nm as identified by CE [19]. The virus batch used in all experiments had a concentration of 5.4 mg/mL, i.e., 6.75×10^{-7} M [20].

Concatemers of five copies of repeat 3 of the ligand binding domain of VLDLR, fused to maltose binding protein (MBP) at the N-terminus and to a his-tag at the C-terminus (MBP-V33333), were produced as described [9,10,13]. Briefly, the plasmid encoding MBP-V3 was cleaved with *Sma*I to generate blunt ends at the 3'end of the sequence encoding the VLDR-repeat. A fragment with the V3 coding sequence produced by PCR was then ligated into this *Sma*I site. Analysis of the plasmids recovered from transformed bacteria showed that concatemers with up to four V3 modules arranged in tandem had formed. MBP-V3333 was again digested with *Sma*I and ligated with a V3 fragment. From the resulting higher order concatemers, MBP-V33333 was selected. The concentration of purified MBP-V33333 used in all experiments was 0.2 mg/mL, corresponding to 29.6×10^{-7} M, as determined with the BCA assay (Pierce, Rockford, IL, USA).

2.2. Complex formation

Virus was mixed with receptor at various molar ratios in sample buffer (50 mM borate, pH 8.3). Five μl of HRV2 at 67.5 or 135 nM was incubated with increasing amounts of MBP-V33333 (5 μl from 0 to 1.48 μM). Complex formation was allowed to occur during incubation at room temperature for 1 h, then the sample was injected and the components were separated by CE.

2.3. Instrumentation

Capillary electrophoresis was performed with an automated HP3D Capillary Electrophoresis System (Agilent, Waldbronn, Germany) equipped with a diode array detector. An uncoated fused silica capillary (Composite Metal Services Ltd., UK) with 60.0 cm total, 51.5 cm effective length, and 50 μm ID was used. The capillary was packed in a standard HP cassette and thermostated to 20.0 °C during all experiments. Injection was at 450 mbar s, voltage was +25 kV. Data acquisition, storage, and analysis were performed using Agilent ChemStation Plus software. The background electrolyte (BGE) for CE separation was 100 mM boric acid containing 10 mM SDS, adjusted to pH 8.3 with 1 M NaOH. Complex formation was carried out in sample borate buffer. *o*-Phthalic acid at 10 μg/ml was used as an internal standard.

3. Results

3.1. Capillary electrophoresis separation of virus–receptor complexes

HRV2, at an initial concentration of 0.68×10^{-7} M in the incubation mixture, was mixed at various ratios with MBP-V33333, a recombinant concatemer of five copies of ligand binding module 3 of VLDLR fused to maltose binding protein. After complex formation for 1 h at room temperature, an aliquot was injected into the capillary and the components were separated by CE. The control incubation, containing virus only, gave rise to a single peak with a net mobility of 20.8×10^{-9} $m^2 V^{-1} s^{-1}$ (Fig. 1, panel A, and Table 1) that roughly agrees with that determined previously for HRV2 [21]. When a mixture containing virus and receptor at a molar ratio of 1:1.1 was analyzed (panel B), a series of peaks with decreasing intensity at longer migration times, i.e., lower total mobility, were seen. Note that this corresponds to a higher net mobility as the anionic analytes migrate against the electroosmotic flow directed towards the cathode. From comparison with panel A, it is apparent that the first main peak (indicated by 0) represents the free virus. The other peaks were tentatively identified as complexes with increasing numbers of receptor molecules bound per virus particle. The tracings obtained at higher ratios of receptor to virus (panel C–G) support this view. Finally, at an excess of receptor of 18 and higher, a single peak, presumably the saturated virus–receptor complex (indicated by '12'), appeared together with the peak corresponding to excess receptor (MBP-V33333). This is similar to earlier results with MBP-V1-3 and MBP-V1-8, where the virus peak broadened and was shifted upon addition of receptor likely reflecting the presence of a population of viral particles with different receptor occupancy; at high receptor to virus ratios, the peak became narrow again reflecting the presence of a single species of virus–receptor complex. In these previous experiments, no resolution of the different complexes was achieved [16]. This might be due to a smaller difference in mobility or to lower affinity leading to partial dissociation during the CE run.

3.2. Electrophoretic mobilities of virus–receptor complexes

Upon increasingly higher occupancy, the net mobility of the individual complexes increased (Table 1). It depends on the

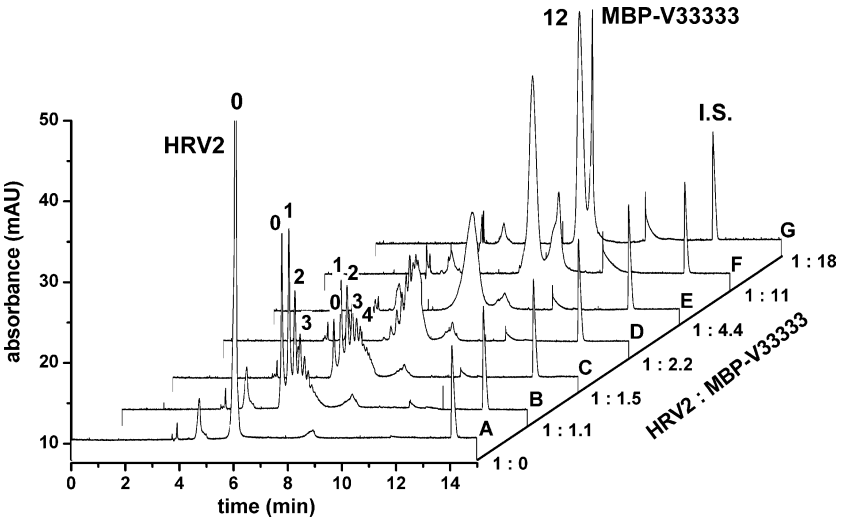

Fig. 1. Capillary electropherograms of complexes between MBP-V33333 and HRV2. In traces A to F, HRV2 at a constant concentration of 0.68×10^{-7} M was incubated with increasing concentrations of receptor (0–7.4×10^{-7} M). Trace G depicts the result for a virus sample with 0.34×10^{-7} M concentration, and an 18-fold molar excess of MBP-V33333. Experimental conditions: uncoated fused silica capillary, 60.0/51.5 cm length, 50 μm I.D.; detection at 200 nm. Voltage +25 kV. Injection 450 mbar s BGE: 100 mM borate buffer, pH 8.3, 10 mM SDS. The numbers of the peaks indicate the occupancy with $n = 1, 2, 3, 4$, etc. receptor fragments. 0: free virus. MBP-V33333: peak of free receptor. Numbers at the *z*-axis are the initial molar ratios of virus to receptor in the incubation mixture. IS, internal standard, *o*-phthalic acid at 10 μg/mL.

Table 1
Net mobilities of virus-receptor complexes

Peak number	0	1	2	3	4	5	6	7	8	9	10	11	12
μ_n	20.82	22.28	23.43	24.36	25.11	25.71	26.25	26.68	27.07	27.43	~27.7	~27.9	~28.2

Net mobilities, μ_n, of the peaks in the electropherograms shown in Fig. 1. The analytes are anions, but are recorded at the cationic side of the separation capillary due to the high electroosmotic flow. Data were corrected by the mobility of the electroosmotic flow. Mobility is in 10^{-9} $m^2 V^{-1} s^{-1}$. Free virus is indicated by number 0, the numbers, *n*, of the consecutive peaks follow the sequence with increasing migration time. Effective mobility of fully saturated complex: 28.16×10^{-9} $m^2 V^{-1} s^{-1}$. Temperature 20 °C. Note that up to number 9 the peaks could be clearly distinguished. The position of the higher order peaks was estimated.

charge to mass ratio. Upon complex formation, the mass is expected to only marginally increase from ~8.1 MDa for the virus [20] to 8.2 MDa for a complex containing 12 molecules of MBP-V33333 ($M_r = 67.4$ kDa). However, an increase in the mass cannot account for the difference in migration since it rather leads to a reduction of the mobility. We have, thus, to assume that a significant modification of the surface charge of the virus takes place upon receptor binding. This agrees well with the known involvement of two lysines, Lys1224 and Lys1228 in the HI loop of VP1, in binding the receptor [12]. The acidic cluster of the receptor module likely neutralizes the positive charge of these lysines; additionally, the carboxylates of the strongly acidic entire molecule including MBP (calculated p*I* of 4.7) might impart a negative charge to the complex. When a single module covers these two lysines within its footprint on the viral surface, 24 positive charges should be lost with a concomitant gain of a number of negative charges. However, presence of SDS micelles and changes of the hydrodynamic diameter of the virus upon receptor binding preclude an exact theoretical assessment. MBP-V33333 has a factor Xa cleavage site between the MBP and the concatemer allowing for separation of MBP from V33333 [9]. When the same experiments were carried out with V33333, from which the MBP had been enzymatically removed, the different complexes were not resolved. MBP is, therefore, largely responsible for the strong modification in migrational behavior in CE.

4. Discussion

4.1. Number of receptors bound to the virus at saturation

In the electropherograms of the complexes formed between MBP-V33333 and HRV2 at low stoichiometric ratio, at least nine complex peaks can be distinguished (Fig. 1, panel C, see also the expanded view in Fig. 4). However, from the shape of the ensemble it is clear that complexes with more than nine receptors are present. Although higher order peaks cannot be fully resolved, it is possible to locate approximately their positions and thus to derive their mobilities. These data are given in Table 1 together with the effective mobility of the fully saturated complex (obtained at a 40-fold molar excess of receptor). The data indicate that the increase in mobility of the subsequent complexes changes with increasing receptor occupancy in a non-linear fashion down to the fully saturated complex. To assess the number of receptors bound at saturation, the differences between the net mobilities of the individual complexes to that of the saturated complex were plotted as a function of the peak number (Fig. 2). According to this approach, peak number 12 indeed approximates the net mobility of the saturated complex. This strongly suggests a stoichiometry of 1:12 in the virus–receptor complex upon occupation of all 12 vertices of the icosahedron with receptor. However, we do not know whether all five sites around the fivefold axis are occupied by receptor modules, since the MBP and a number of amino acid residues that have been introduced between the

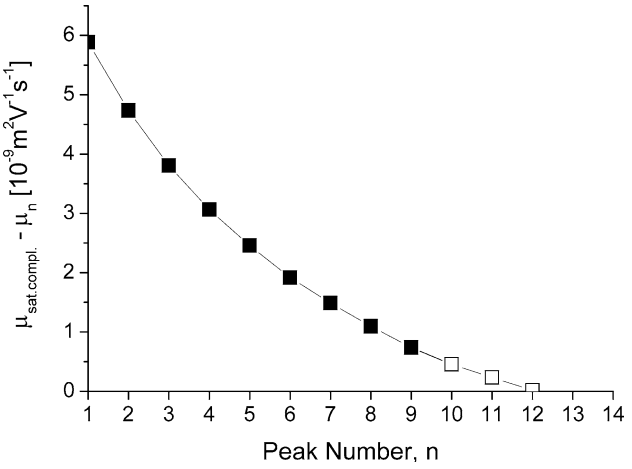

Fig. 2. Difference of net mobility between consecutive peaks and saturated species versus peak number. For numbering of peaks see Fig. 1, mobilities, see Table 1. Filled squares, clearly recognizable peaks; empty squares, estimated peaks.

C-terminus of the last module and the his-tag by the cloning procedure might result in steric hindrance. This question might be settled by comparing the binding affinities of MBP-V33333 with that of a construct in which all residues not belonging to the receptor modules have been removed. Fluorescence resonance energy transfer between a fluorophore attached to the N-terminus and a fluorophore attached to the C-terminus of such a construct would also indicate that the receptor adopts a ring-like structure upon binding to the virus (see Fig. 5).

Fig. 1 shows that the peak corresponding to free receptor (migrating after the complex) appeared already at virus receptor ratios that did not result in saturation. This might be due to the presence of inactive receptor that cannot bind to the virus. V33333 contains altogether 15 individual disulfide bonds that need to assemble correctly out of the theoretical 6×10^{15} possibilities. Free receptor would also be present if the equilibrium association constant were unfavorably low (see below). Notwithstanding these limitations, the binding stoichiometry can be determined from the mobilities of the complex peaks as described (see Fig. 2). This is especially so because from the geometry of the virus only multiples of 12 need to be considered (see Fig. 5).

4.2. Equilibrium concentration of the individual complexes

We tried to calculate the theoretical distribution of the complexes formed between the receptor fragments and the virus assuming 12 binding sites. For this, an approximate value for the equilibrium association constants is required. As the equilibrium is shifted towards the free components when a twofold diluted sample containing virus and receptor at a molar ratio of 1:2.2 (compare Fig. 3A and B) is analyzed, it becomes clear that the complex constant must lay within the high nanomolar range, as are the concentrations of the reactants. It should also be mentioned that, due to partial dissociation of the complexes in the mixture, the determination of the stoichiometry by the usual binding curves would be erroneous. This might be overcome by using higher concentrations of the reactants; however, this was not possible due to limitations in sample preparation and solubility of the components.

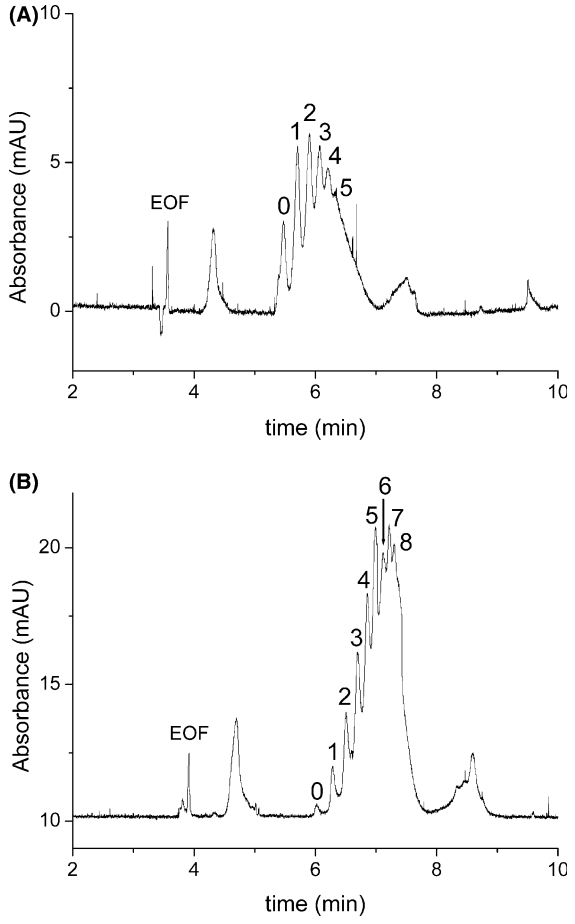

Fig. 3. Electropherogram (A) obtained upon complex formation with the twofold diluted sample (virus concentration 0.34×10^{-7} M) compared to the sample shown in Fig. 1D. For both samples, the initial molar ratio of virus to receptor is 1:2.2. (B) Extended view of trace D from Fig. 1 for better comparison. EOF: position of the electroosmotic flow marker. The numbers indicate the occupancy of the virus with 1, 2, 3, etc. receptors. 0: free virus.

Complex formation between soluble receptors and virus was allowed to occur in the absence of SDS but the background electrolyte used for CE separation contained 10 mM SDS. The detergent was found to be required to avoid extensive adsorption of the virus to the capillary wall [19] and below 5 mM no reliable electropherograms were obtained (not shown). Although the complexes are exposed to SDS only for some few minutes during the analysis, the detergent might compete for the binding sites during the CE run and thereby prevent reassociation of dissociated complexes. This is possibly the reason for the slight change of the electropherograms as seen upon reduction of the SDS concentration in the background electrolyte from 10 to 5 mM; this resulted in a marginal decrease of the peak area of the free virus with a concomitant increase of the peak areas of the complexes. However, electropherograms recorded in the presence of SDS at concentrations between 10 and 50 mM were virtually identical (data not shown). For the reason pointed out above, the affinity constants measured by CE cannot be considered the "true" values and they might be different when determined by other methods.

To derive the equilibrium concentrations of the individual complexes, the law of mass action was applied to the equilibria

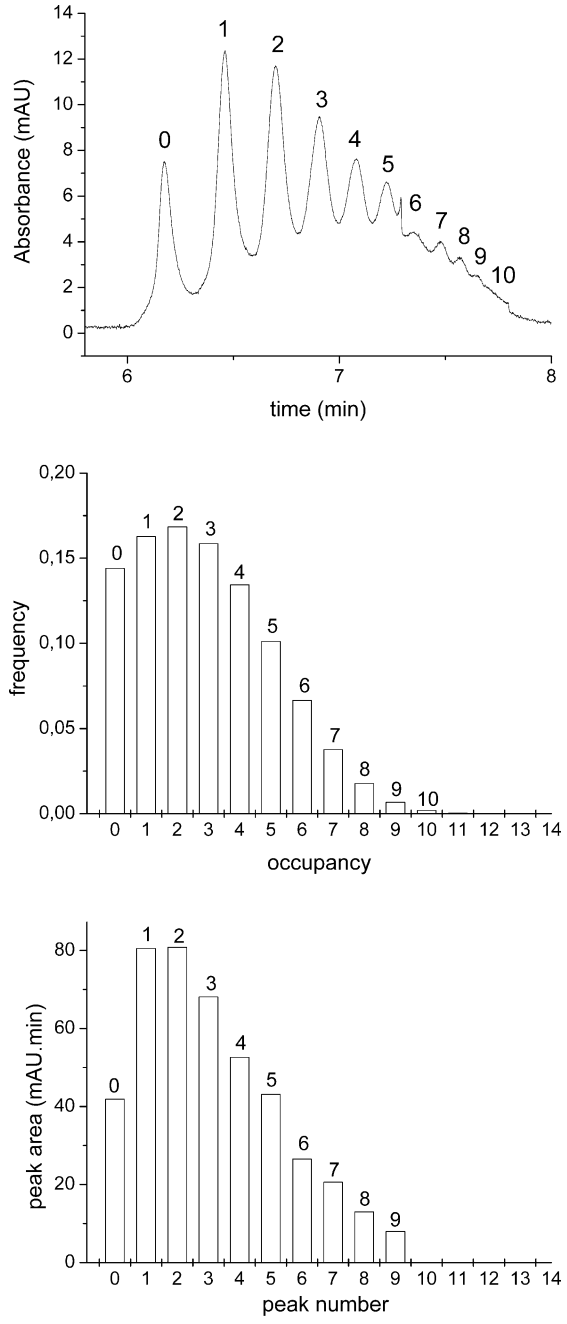

Fig. 4. Comparison of the CE separation of HRV2-receptor complexes (upper panel) with the results of a calculation of the distribution of the species according to Eq. (4) (middle panel). Lower panel, histogram of the areas of the peaks in the electropherogram shown in the top panel. Initial molar ratio of virus: receptor is 1:1.5 in the incubation mixture. First peak (number 0) corresponds to free virus; the following peaks correspond to complexes with different receptor occupancies as indicated by the numbers. Experimental conditions as in Fig. 1. Assumptions for calculation: virus concentration 1×10^{-7} M, receptor concentration 3×10^{-7} M. Complex constants for the 12 binding sites decreasing by 1×10^{-7} each from $K_1 = 12 \times 10^{-7}$ M to $K_{12} = 1 \times 10^{-7}$ M.

between the virus, A, and the receptor fragments, B. Formation of complex with one receptor according to $A + B = AB_1$ is described by the association constant $K_1 = [AB_1]/[A][B]$, whereby the brackets indicate the concentrations at equilibrium. The equilibrium concentration of the complex AB_1 is thus $[AB_1] = K_1 \cdot [A][B]$.

Extending this approach to the general case $AB_{(n-1)} + B = AB_n$, we can formulate accordingly

$$[AB_n] = K_1 K_2 \cdots K_n \cdot [A][B]^n = \left\{ \prod_1^n K_n \right\} [A][B]^n. \quad (1)$$

Here, we assume that the constants for the formation of the individual species are not equal. For equal complex constants, K, the term $\{\prod_1^n K_n\}$ is equal to K^n.

Note that all concentrations in the equations are equilibrium concentrations. The dependence of $[AB_n]$ as a function of the initial reactant concentrations of virus (A) and of receptor (B) is obtained as follows. Due to the conservation of mass, the following equations must be valid

$$[A] = (A) - [AB_1] - [AB_2] - \ldots - [AB_k] = (A) - \sum_1^k [AB_k], \quad (2)$$

$$[B] = (B) - [AB_1] - 2[AB_2] - \ldots - k[AB_k] = (B) - \sum_1^k k[AB_k], \quad (3)$$

where k is the number of receptor binding sites, in our case we assume 12.

The concentration of the individual species as a function of K_n, and the initial concentrations (A) and (B) are thus:

$$[AB_n] = \left\{ \prod_1^n K_n \right\} \left\{ (A) - \sum_1^{12} [AB_k] \right\} \left\{ (B) - \sum_1^{12} k[AB_k] \right\}^n \quad (4)$$

and the occupancy of n can take the values $1, 2, 3, \ldots, 12$.

The concentrations of the individual complexes as a function of the initial concentrations of virus and receptor, and for particular complex constants were obtained by using the software Gepasi [22]. Assuming an identical complex constant for all reactions failed to match the pattern of the concentrations of the complexes found experimentally, since regardless of the initial virus – receptor ratios used as an input no maximum concentration at a medium occupancy (see Fig. 1C–E) was obtained.

A distribution closely fitting the experimental data was obtained under the reasonable assumption that the on-rate of the reaction was decreasing with increasing occupancy, since the probability of collision that leads to a binding event is decreased. This means that the individual equilibrium state is entropically determined (it is reasonable that the enthalpy of binding to the individual independent sites is most probably equal, since their distance on the viral surface excludes steric hindrance; see Fig. 5). The entropy is related to the probability of each state being realized, which is connected to the number of free sites on the virus surface. This number is 12 for free virus and decreases by one for each consecutively bound receptor. This means that the probability decreases from 12/12 to 1/12 and the entropy increases proportional to $\ln(1/12)$ for each step. Consequently, the binding constants decrease by 1/12 of K_1 for each consecutive complex. Based on this postulation, calculations were carried out and in the example shown below K_1 was set to 12×10^{-7} M with the constants decreasing by 1×10^{-7} M for each of the higher order complexes (K_2 is thus 11×10^{-7} M, K_3 is 10×10^{-7} M, etc.). The initial virus

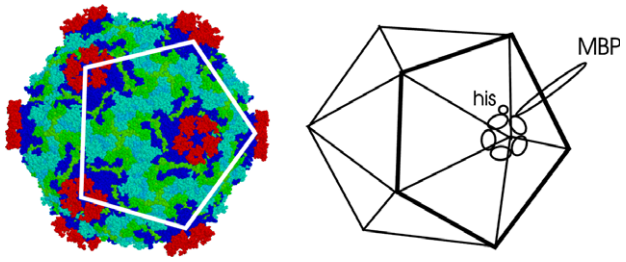

Fig. 5. Model of HRV2–receptor complexes. Space filling representation of the complex between V23 and HRV2 as deduced from the X-ray structure (12). Left panel: five single V3 modules (red) are attached to the five symmetry related sites at the 12 vertices of the icosahedral viral capsid interacting exclusively with VP1 (blue). This results in 60 modules attached in total. Note the possibility of simultaneous attachment of V2 and V3, since the occupancy is only 80% (12). Upon concatenation, five modules within a single molecule could adopt a similar structure but with only 12 molecules bound per virion. In this arrangement, the MBP and the hexa-his tag (his) are predicted to come close to each other as schematized in the right panel. One of the 12 pentamers making up the viral capsid is indicated with a thick line.

concentration was 1×10^{-7} M and the calculation was carried out for a threefold molar excess of receptor over virus.

The distribution of the concentrations of the complexes obtained under these circumstances is shown in Fig. 4, middle panel. It can be seen that non-reacted virus (indicated by 0) is still present, and the histogram has a maximum at an occupancy of $n = 2$, then it falls off with a complex containing 10 receptors which are still recognizable. This distribution rather closely resembles that experimentally obtained with a receptor excess of 1.5. Taking into account the complexity of this virus–receptor system and the rough approximation of the values used in the calculation, we believe that the agreement between experiment and calculation is remarkable.

As suggested by the structure of the complex between V23 and HRV2 solved by X-ray crystallography (Fig. 5), we have presented evidence that a concatemer of five consecutive copies of repeat 3 of the VLDL-receptor can attach to the 12 vertices of the icosahedral capsid of human rhinovirus serotype 2. This most probably results in a ring-like structure wound around each fivefold axis as schematized in Fig. 5. In this arrangement more than one and possibly all five modules of a single molecule attach simultaneously to the virus. Similarly, the natural receptors LDLR, VLDLR, and LRP might contribute with up to five modules to virus binding giving rise to a similar conformation.

Acknowledgements: This work was supported by the Austrian Science Foundation (Project P15667). We thank Irene Goesler for the preparation of the viruses, Stephane Nizet for providing MBP-V33333, Peter Chiba for helpful discussions and for drawing our attention to the program Gepasi, Gottfried Köhler for critical comments, and the Austrian Exchange Service (CEEPUS network H-76) for a grant to T.K.

References

[1] Semler, B.L. and Wimmer, E. (2002) in: Molecular Biology of Picornaviruses (Semler, B.L. and Wimmer, E., Eds.), ASM Press, Washington, DC.
[2] Uncapher, C.R., Dewitt, C.M. and Colonno, R.J. (1991) Virology 180, 814–817.
[3] Savolainen, C., Blomqvist, S., Mulders, M.N. and Hovi, T. (2002) J. Gen. Virol. 83, 333–340.
[4] Nykjaer, A. and Willnow, T.E. (2002) Trends Cell Biol. 12, 273–280.
[5] Hofer, F., Gruenberger, M., Kowalski, H., Machat, H., Huettinger, M., Kuechler, E. and Blaas, D. (1994) Proc. Natl. Acad. Sci. USA 91, 1839–1842.
[6] Marlovits, T.C., Abrahamsberg, C. and Blaas, D. (1998) J. Virol. 72, 10246–10250.
[7] Strickland, D.K., Kounnas, M.Z. and Argraves, W.S. (1995) FASEB J. 9, 890–898.
[8] Snyers, L., Zwickl, H. and Blaas, D. (2003) J. Virol. 77, 5360–5369.
[9] Ronacher, B., Marlovits, T.C., Moser, R. and Blaas, D. (2000) Virology 278, 541–550.
[10] Neumann, E., Moser, R., Snyers, L., Blaas, D. and Hewat, E.A. (2003) J. Virol. 77, 8504–8511.
[11] Hewat, E.A., Neumann, E., Conway, J.F., Moser, R., Ronacher, B., Marlovits, T.C. and Blaas, D. (2000) EMBO J. 19, 6317–6325.
[12] Verdaguer, N., Fita, I., Reithmayer, M., Moser, R. and Blaas, D. (2004) Nat. Struct. Mol. Biol. 11, 429–434.
[13] Moser, R., Wruss, J., Snyers, L., Peters, H., Peters, T. and Blaas, D. (2004) in preparation.
[14] Marlovits, T.C., Zechmeister, T., Gruenberger, M., Ronacher, B., Schwihla, H. and Blaas, D. (1998) FASEB J. 12, 695–703.
[15] Marlovits, T.C., Abrahamsberg, C. and Blaas, D. (1998) J. Biol. Chem. 273, 33835–33840.
[16] Okun, V.M., Moser, R., Ronacher, B., Kenndler, E. and Blaas, D. (2001) J. Biol. Chem. 276, 1057–1062.
[17] Jeon, H. and Shipley, G.G. (2000) J. Biol. Chem. 275, 30458–30464.
[18] Rueckert, R.R. (1976) in: Comprehensive Virology (Fraenkel-Conrad, H. and Wagner, R.R., Eds.), Vol. 6, pp. 131–213, Plenum Press, New York.
[19] Okun, V.M., Ronacher, B., Blaas, D. and Kenndler, E. (1999) Anal. Chem. 71, 2028–2032.
[20] Bacher, G., Szymanski, W.W., Kaufman, S.L., Zollner, P., Blaas, D. and Allmaier, G. (2001) J. Mass Spectrom. 36, 1038–1052.
[21] Okun, V., Ronacher, B., Blaas, D. and Kenndler, E. (2000) Anal. Chem. 72, 2553–2558.
[22] Mendes, P. and Kell, D. (1998) Bioinformatics 14, 869–883.